

# ResORR: A Globally Scalable and Satellite Data-driven Algorithm for River Flow Regulation due to Reservoir Operations

Pritam Das<sup>1</sup>, Faisal Hossain<sup>1\*</sup>, Sanchit Minocha<sup>1</sup>, Sarath Suresh<sup>1</sup>, George K. Darkwah<sup>1</sup>, Hyongki Lee<sup>2</sup>, Konstantinos Andreadis<sup>3</sup>, Miguel Laverde-Barajas<sup>4</sup> and Perry Oddo<sup>5</sup>

<sup>1</sup>Department of Civil and Environmental Engineering, University of Washington, Seattle, WA, USA

<sup>2</sup>Department of Civil and Environmental Engineering, University of Houston, Houston, TX, USA

<sup>3</sup>Department of Civil and Environmental Engineering, University of Massachusetts, Amherst, MA, USA

<sup>4</sup>Asian Disaster Preparedness Center, Bangkok, 10400, Thailand

<sup>5</sup>Science Systems and Applications, Inc., Lanham, MD, USA

**Abstract:** We propose a globally scalable algorithm, ResORR (Reservoir Operations driven River Regulation), to predict regulated river flow and tested it over the heavily regulated basin of the Cumberland River in the US. ResORR was found able to model regulated river flow due to upstream reservoir operations of the Cumberland River. Over a mountainous basin dominated by high rainfall, ResORR was effective in capturing extreme flooding modified by upstream hydropower dam operations. On average, ResORR improved regulated river flow simulation by more than 50% across all performance metrics when compared to a hydrologic model without a regulation module. ResORR is a timely software algorithm for understanding human regulation of surface water as satellite-estimated reservoir state is expected to improve globally with the recently launched Surface Water and Ocean Topography (SWOT) mission.

**Keywords:** River Regulation, Reservoir Operations, Hydrological Modeling, Satellite Remote Sensing

1  
2  
3  
4  
5  
6  
7  
8  
9  
10  
11  
12  
13  
14  
15  
16  
17  
18  
19  
20  
21  
22  
23  
24  
25  
26  
27  
28  
29  
30  
31  
32  
33  
34  
35  
36  
37  
38  
39  
40  
41  
42  
43  
44  
45  
46  
47  
48  
49  
50  
51  
52  
53  
54  
55  
56  
57  
58  
59  
60  
61  
62  
63  
64  
65

**Highlights:**

- A globally scalable algorithm, called ResORR, to predict regulated flow from naturalized flow and upstream reservoir storage is proposed.
- ResORR requires globally available satellite-based reservoir storage and satellite-forced hydrologic model.
- ResORR was tested on the heavily regulated river basin of the Cumberland river in Tennessee, USA.
- On average, ResORR improved regulated river flow simulation by more than 50% across all performance metrics when compared to a hydrologic model without a regulation module.
- ResORR is a timely software algorithm that can be further improved of its skill with reservoir storage data from the Surface Water and Ocean Topography (SWOT) mission.

**Data and Software Availability:** The model code developed during this study is available on GitHub (<https://github.com/UW-SASWE/ResORR>) under the MIT license. Documentation on ResORR is available at - <https://resorr.readthedocs.io/en/latest/>? The github repository was created by first author Pritam Das (pdas477@uw.edu). Author’s experimental CPU environment used Linux Ubuntu OS, Intel Xeon Scalable Gold 6242 at 2.8GHz (16-Core), 192GB RAM.

# 1. Introduction

Rivers have provided humans with food, water and energy security since human civilization first started to take shape in ancient valleys of Tigris-Euphrates, Indus and Nile rivers. This has only been made possible by means of control structures such as dams and reservoirs, which allow storage and release of water from the river according to human needs. Usually, water from the river is stored in reservoirs when the river naturally has higher flows, resulting in a net reduction in the downstream flow of the river. This storage is driven by human needs such as flood control or to meet future freshwater demand when natural availability may be insufficient. The converse happens during naturally occurring periods of low flows, when release of water from reservoirs artificially increases the downstream flow rate during the dry season to meet demand for water. This regulation of surface water, in the form of alteration of the streamflow from its natural pattern of discharge under pristine conditions, can be termed as river regulation.

River regulation can change how the basin responds to a hydro-meteorological event in the form of precipitation or snowmelt, affecting its natural variability and streamflow timing. For instance, Wisser and Fekete (2009) found that the average residence time has increased by 42 days globally over the past century due to construction of reservoirs. Such disruption and alteration of natural conditions is even more profound at a regional scale, for instance, Bonnema and Hossain, (2017) note about 11-30% streamflow alteration in the Mekong basin, with the residence time of reservoirs varying from 0.09 to 4.04 years. Vu et al., (2021) estimate that reservoirs in the Mekong hold 50% of its dry season flow and 83% of its wet season flow. As a result, the high flows of the Mekong-river have reduced by 31%, while the low-flows have increased by 35%.

River regulation can also have serious ecological repercussions. For instance, the unique annual flow reversal of the Tonle Sap River (TSR) leading to filling up the Tonle Sap Lake (TSL) during the wet season and draining it during dry season may cease to exist if the flood pulse of the Mekong River dampens by 50% and is delayed by a month (Pokhrel et al., 2018). The absence of this unique flow reversal may have a negative impact on aquatic biodiversity, particularly for fisheries and paddy planting (Marcaida et al., 2021). Similarly, in European rivers, high-flows appear to be down by 10% while low-flows are up by 8% (Biemans et al., 2011). Negative consequences are not limited to only ecological aspects but can also influence the regional demand-and-supply of resources, with the potential to escalate pre-existing water conflicts. The construction and filling up of the Grand Ethiopian Renaissance Dam (GERD) on the Nile River has been a source of contention between Ethiopia and the other riparian countries – Egypt and Sudan. Eldardiry and Hossain, (2021) estimate that if unprepared, the High Aswan Dam (HAD) – a dam of existential importance to Egypt for its water-food-energy security – may take anywhere from 2 years to 7 years to fully recover following the filling-up of the GERD. Although, they also optimistically estimate that with cooperation and planning between the riparian countries, the recovery period can be limited to immediate 2 years.

Apart from the direct alteration of streamflow timing of rivers, regulation due to dam and reservoir operations can have an indirect effect on other components of the eco-system. For instance, river regulation disturbs the natural sediment flow, resulting in a net reduction in sediment deposition along shorelines of rivers, estuaries and oceans (Dunn et al., 2019; Li et al., 2021). River water temperature anomalies owing to thermal stratification in reservoirs have also been widely recognized (Ahmad et al., 2021; Cheng et al., 2020). Considering the sensitivity of aquatic life to the water temperature changes (Caissie, 2006), river regulation can negatively affect

1  
2  
3  
4 91 the environmental suitability for aquatic organisms (Cheng et al., 2022). Such negative  
5 92 environmental consequences are a direct result of human decisions – which many consider  
6 93 necessary to support the demands of a rapidly growing population. A better understanding of  
7 94 human regulation of river flow, exacerbated by a changing climate and increasing freshwater  
8 95 demand, is urgently required to ensure a sustainable future.

10  
11 96 The coupled nature of human-water resources has led to developments in explicitly  
12 97 modeling reservoir operations in Large-Scale Hydrological Models (LHMs) and Global  
13 98 Circulation Models (GCMs) (Hanasaki et al., 2018; Wada et al., 2017). Existing methods to  
14 99 represent human activities in hydrological models rely on modeling the optimal reservoir release  
15 100 based on operating parameters such as the design role of the reservoir (Hanasaki et al., 2006), land-  
16 101 water management schemes, downstream demand for water and energy (Alcamo et al., 2003;  
17 102 Biemans et al., 2011; Haddeland et al., 2006; Vanderkelen et al., 2022). Many of these human  
18 103 activities are often assumed or ‘parameterized’ due to lack of sufficient observational data on  
19 104 reservoir operations. Using such a parameterized approach, Zhou et al. (2016) found that in highly  
20 105 regulated basins, such as the Yellow and the Yangtze rivers, the seasonal reservoir storage  
21 106 variations can contribute up to 72% of the variability of the basin’s total storage. While such key  
22 107 insights can be obtained using generic schemes of reservoir operations, the underlying assumption  
23 108 of optimal reservoir operations may not always hold true. Stakeholders and reservoir managers  
24 109 must often deviate from optimal operating conditions based on a variety of reasons, such as  
25 110 adapting to regional water and energy demands, new hydro-political reality, environmental  
26 111 regulations, and changing weather and climate patterns that result in river flow to exceed the  
27 112 bounds of pre-dam historical flow records.

30  
31  
32 113 In the past, modeling human decisions of reservoir operations using parameterizations or  
33 114 criteria-based assumptions has been the primary way for characterizing river-regulation due to a  
34 115 lack of publicly available observations on dam operations. However, to better understand river  
35 116 regulation, which is representative of the intricacies of operation of individual reservoirs, we need  
36 117 to characterize and quantify river regulation grounded in observations of reservoir operations  
37 118 (Biswas et al., 2021; Das et al., 2022; Zhou et al., 2016). Earth observing satellites, with their  
38 119 vantage of space and a multi-decadal record of observations on reservoir operations now provide  
39 120 an opportunity to fill this data availability gap by inferring reservoir operations from space  
40 121 (Bonnema & Hossain, 2017).

41  
42  
43 122 Studies have used satellite remote sensing-based reservoir operations monitoring  
44 123 techniques to model the resulting regulation of streamflow. Reservoir releases are obtained by  
45 124 typically assuming water mass balance at the reservoirs, by modeling the inflow and storage  
46 125 change of the reservoirs. For instance, Yoon & Beighley, (2015) and Yoon et al., (2016) model  
47 126 the inflow at reservoirs in the Cumberland basin due to surface runoff and upstream releases using  
48 127 the Hillslope River Routing (HRR) model. The storage change is estimated using historical record  
49 128 of reservoir operations by Yoon & Beighley, (2015) and by simulating SWOT-like storage change  
50 129 estimates by Yoon et al., (2016). The performance of the simulated discharges in both cases  
51 130 improves with the inclusion of reservoirs. Han et al., (2020) also take the approach of simulating  
52 131 reservoir operations by deriving the operating curve of reservoirs using satellite observations.  
53 132 Reservoir releases from upstream reservoirs were added to the inflow of downstream reservoirs in  
54 133 a cascade reservoir system in the Mekong River basin. However, in this case the inclusion of  
55 134 upstream releases did not improve the performance of regulated streamflow estimates drastically.  
56 135 Dong et al., (2023) use historical satellite observations of reservoir water level to calibrate

1  
2  
3  
4 136 parameters of a reservoir operation scheme. The reservoir releases are routed downstream using  
5 137 the Coupled Land Surface and Hydrologic Model System (CLHMS). All the existing studies rely  
6 138 on specific hydrological routing models to route the runoff and releases downstream. There doesn't  
7 139 exist a method to leverage existing hydrological model setups, that are usually calibrated using  
8 140 data that is only accessible to local stakeholders. Furthermore, the availability of high frequency  
9 141 satellite observations near-real time provides an opportunity to move away from parameterization  
10 142 and simulation driven estimation of reservoir operations to a direct observation-based approach  
11 143 for modeling reservoir releases. Rather than relying on parameterized or criteria-based  
12 144 assumptions of reservoir operations, we can now use actual observation-based reservoir operations  
13 145 to quantify the regulation of flow in physical models. Because satellite observations today can  
14 146 track the dynamic state of reservoirs comprising surface area, water surface elevation,  
15 147 evapotranspiration losses, storage change and even outflow (Cooley et al., 2021; Hossain et al.,  
16 148 2017; Lee et al., 2010; Okeowo et al., 2017; Zhao et al., 2022), there is now a stronger argument  
17 149 to move away from assumptions and parameterizations in representing human flow regulation in  
18 150 physical hydrologic models.

23 151         Satellites such as the Landsat, Sentinel, and Jason series have been extensively monitoring  
24 152 hydrologically relevant aspects of the Earth's surface, such as surface reflectance and elevation, at  
25 153 the global scale. For instance, Gao et al., (2012) were able to recreate storage variations of large  
26 154 reservoirs using observations from the Moderate Resolution Imaging Spectroradiometer (MODIS)  
27 155 satellite platform. Cooley et al., (2021) used NASA's ICESat-2 satellite observations of water level  
28 156 height to estimate that about 3/5<sup>th</sup> of the Earth's surface water storage variability takes place due  
29 157 to reservoirs. Moreover, the recently launched terrestrial hydrology-focused Surface Water and  
30 158 Ocean Topography (SWOT) satellite is now expected to improve the monitoring of surface water  
31 159 resources at an unprecedented scale and accuracy (Biancamaria et al., 2016). Together, these  
32 160 Earth-observing satellites provide an opportunity to independently track various aspects of the  
33 161 hydrological cycle, including reservoir operations (Bonnema & Hossain, 2017; Hossain et al.,  
34 162 2017). Using multi-sensor satellite data on surface water, we can now build comprehensive,  
35 163 distributed, and scalable modeling platforms to simulate reservoir-river systems. The Reservoir  
36 164 Assessment Tool (RAT) is one such modeling platform that can estimate reservoir fluxes,  
37 165 comprising inflow to the reservoir, storage change, evaporative losses and outflow, solely using  
38 166 satellite data and hydrological modeling (Biswas et al., 2021; Das et al., 2022). More recent  
39 167 developments have made it easier to monitor reservoirs using RAT, further democratizing the  
40 168 availability of surface water data at the granular level for regulated river systems (Minocha et al.,  
41 169 2023). This has allowed for both global and regional scale studies of the anthropogenic impact on  
42 170 terrestrial water storage (Biswas & Hossain, 2022) and floods (Suresh et al., 2024), especially in  
43 171 the regions of the world that lack a robust data collection and sharing infrastructure.

49 172         Considering the importance and urgency of an observations-driven understanding of river  
50 173 regulation, there is now a need to develop methods to quantify river regulation due to reservoir  
51 174 operations that can be scaled globally based on publicly and globally available satellite  
52 175 observables. The wide availability of satellite-based reservoir operations data will only keep  
53 176 increasing with the recent launch of the SWOT mission that is optimized for surface water tracking,  
54 177 particularly for lakes and reservoirs. Here, the multi-satellite observations used by RAT to estimate  
55 178 storage change (Das et al., 2022) can be directly used as observations to quantify river regulation,  
56 179 obviating the need to separately model reservoir operations based on parameterizations or  
57 180 operating assumptions, which can be both difficult and unrepresentative of actual reservoir  
58 181 operations. Given the availability of multi-decadal satellite observations of surface water that are

1  
2  
3  
4  
5  
6  
7  
8  
9  
10  
11  
12  
13  
14  
15  
16  
17  
18  
19  
20  
21  
22  
23  
24  
25  
26  
27  
28  
29  
30  
31  
32  
33  
34  
35  
36  
37  
38  
39  
40  
41  
42  
43  
44  
45  
46  
47  
48  
49  
50  
51  
52  
53  
54  
55  
56  
57  
58  
59  
60  
61  
62  
63  
64  
65

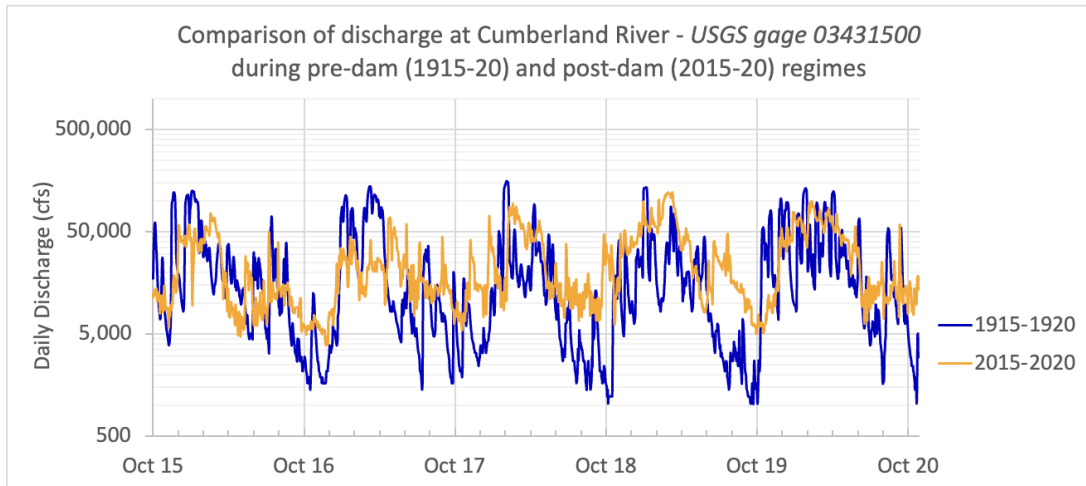
182 now made widely accessible due to advancements in information technology, we are now uniquely  
183 positioned to predict regulated flow at a level of granularity that was not possible before.  
184 Estimation of river regulation grounded in observational data inherently represents the actual or  
185 likely decisions made by reservoir operators. The primary research question that this paper  
186 addresses is – *How can river regulation due to operation of reservoirs be formulated in a globally*  
187 *scalable format using primarily satellite observations?* The objectives of the paper are as follows:

1. To develop a globally scalable river-regulation algorithm based on satellite observables or satellite derived reservoir data for predicting the human regulation of surface water.
2. To investigate incorporation of the river-regulation algorithm in the RAT modeling platform for regulated rivers, and quantify its skill in capturing river flow regulation at a basin scale.

## 2. Study area and Data

### 2.1. The Cumberland River in Tennessee, US

The Cumberland River is highly regulated by a system of 10 major dams and reservoirs with varying primary use cases, making it one of the most heavily regulated basins. The United States Army Corps of Engineers (USACE) Nashville District, own and operate 10 such multi-purpose dam/reservoir projects on the Cumberland River, with the first dams being built in 1950s. These dams are used for hydropower generation, flood control, recreation, commercial navigation, public water supply, and fisheries and wildlife management – bringing in immense economic benefits to the region (Robinson, 2019). Figure 1 compares the daily discharge in the Cumberland River for two time-periods corresponding to unregulated conditions (1916-1920) and regulated conditions (2016-2020). The effect of regulation can be clearly seen in the figure, in the form of reduced range and variability in the discharge hydrograph. Studies suggest that such regulation has caused a sharp decline in the population and species variety of Mussels in the basin, which were plentiful when the river was unregulated (Neel & Allen, 1964; Tippit et al., 1995; Wilson & Clark, 1914). In addition to the highly regulated status of the basin, the availability of long periods of in-situ observational data from the operating agencies makes this basin an ideal test bed for investigating anthropogenic river regulation (Bonnet et al., 2015).



210  
211 Figure 1: Comparison of 5 years of daily discharge during (a) unregulated conditions, prior to  
212 construction and operation of major dams (1916-1920), and (b) regulated conditions, as observed  
213 in the Cumberland River near Nashville, TN. The flow rate in a regulated regime has a markedly  
214 attenuated peak-trough range – with low flows rarely dropping below 5000 cfs as compared to  
215 the unregulated regime when flow rates naturally used to drop to 1000 cfs. Source: United States  
216 Geological Survey (USGS).

217  
218 Originating in the Appalachian Mountains, the Cumberland River flows westwards  
219 through the states of Kentucky and Tennessee in the United States, draining a region of about  
220 18,000 sq. miles (~45,000 sq. km), before merging into the Ohio River. Ten dams – Martins Fork,  
221 Laurel, Wolf Creek, Dale Hollow, Cordell Hull, Center Hill, Old Hickory, J. Percy Priest,  
222 Cheatham, and Barkley dams – are operated by USACE, with some additional dams operated by  
223 the Tennessee Valley Authority (TVA) (Robinson, 2019). Limited by the availability of in-situ  
224 reservoir operations data, 8 of the USACE owned dams were included in this study. Based on the  
225 conclusions of the study, the authors believe that the results are not affected by the exclusion of  
226 the 2 USACE dams owing to their relatively insignificant (Martin’s Fork dam) to no storage  
227 (Cheatham dam). The region generally has a temperate, warm, and humid climate, with most of  
the precipitation occurring from December through May.

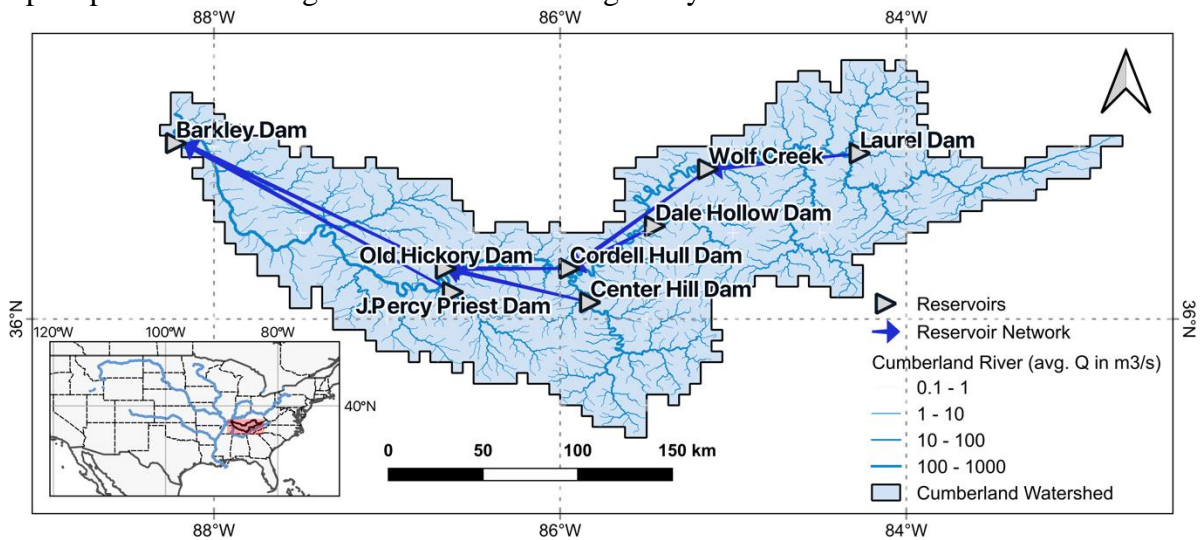


Figure 2: Map of the Cumberland basin, showing locations of the reservoirs, the reservoir network and the location of the Cumberland basin in the US.

## 2.2. In-situ and satellite observations of reservoir dynamics

To develop, test and validate the river-regulation algorithm, observed in-situ data pertaining to reservoir operations – inflow, outflow, and storage – were used, which were obtained from the ResOpsUS (Steyaert et al., 2022) dataset. This dataset is a compilation of in-situ reservoir operations data for 679 major dams in the US, including 8 of the USACE dams in the Cumberland basin and one dam operated by the TVA, until November 2019. Daily storage change was calculated using the storage values in the dataset for all but 2 dams – Old Hickory and J. Percy Priest – which had missing storage data from July 2015 onwards. The storage change for these reservoirs were obtained by subtracting the reported Outflow from the Inflow ( $\Delta S = I - O$ ). Readers are referred to section 7.2 for more discussion on this data preparation step. The in-situ data was also used to force the river-regulation model in certain experiments to compare the sensitivity of the river-regulation model to the accuracy of input data – a detailed discussion is provided in section 4.1. Additionally, the in-situ Area-Elevation Curve (AEC) of all the USACE reservoirs were also obtained from the Access to Water Resources Data – Corps Water Management System (CWMS) Data Dissemination tool (USACE, n.d.).

The latest version of Reservoir Assessment Tool (RAT 3.0) was used to obtain the storage change and river flow under pristine (naturalized) conditions (assuming no upstream reservoirs). Originally developed by Biswas et al., (2021), the RAT framework is designed to improve access to information on reservoir dynamics, especially with recent developments leading to both a higher performance and accessibility (Das et al., 2022; Minocha et al., 2023). Using the default hydrological model of RAT, Variable Infiltration Capacity (VIC) (Liang et al., 1994), rainfall-runoff modeling was performed at a  $0.0625^\circ$  spatial resolution. The inflow to each reservoir’s location under natural conditions was estimated using the VIC-Routing model (Lohmann et al., 1998), which uses the linearized Saint-Venant equation to route streamflow within the watershed. The default VIC parameters, and sources of temperature and wind data used in RAT 3.0 were used to force the hydrological model. The precipitation was obtained from the ERA-5 reanalysis dataset (Hersbach et al., 2020). It must be noted here that the VIC-based reservoir inflow in RAT 3.0 does not take upstream reservoir operations into account, and hence the need to develop a model that can supplement the RAT framework by taking upstream regulation into consideration. A detailed discussion on how the hydrological model’s estimated inflow in pristine conditions is used in the river regulation model can be found in section 3.1. Since the in-situ AEC of the TVA-owned reservoir was not available, the default AEC option in RAT 3.0 was applied based on the Shuttle Radar Topography Mission Digital Elevation Model (SRTM DEM) (Earth Resources Observation And Science (EROS) Center, 2017).

## 3. Methods

### 3.1. Reservoir Operations driven River Regulation (ResORR) – Conceptual algorithm

The core assumption of the ResORR algorithm is that the volume of water entering the reservoir, Inflow (I), is composed of two components – natural and regulated. The Natural Runoff

(NR) is defined as the component of surface runoff that flows naturally into the reservoir without passing through any upstream reservoirs. Similarly, the Regulated Runoff (RR) is the component of surface runoff that first gets intercepted by an upstream reservoir before being released based on the reservoir's operations policy. The partitioning of the inflow to a reservoir is defined by the following equation,

$$I = NR + RR \quad (1)$$

Essentially, the problem of estimating the inflow at any reservoir is decomposed into the two parts of estimating the natural and regulated components of the incoming streamflow. A detailed discussion on estimating these sub-components of inflow is provided later in the section. The estimated inflow to a reservoir in this scheme will, hence, be affected by regulation due to upstream reservoir operations.

For example, consider the example of a two-reservoir system (A and B), where reservoir B is downstream of reservoir A, depicted in the schematic in Figure 3(a). In this scenario, the inflow at reservoir B would have contributions from the outflow of the upstream reservoir A in the form of RR (i.e.,  $RR \neq 0$ ), in addition to the NR. On the other hand, since reservoir A has no upstream reservoirs, the inflow to the reservoir would be fully natural, i.e.,  $RR = 0$  and  $I = NR$ .

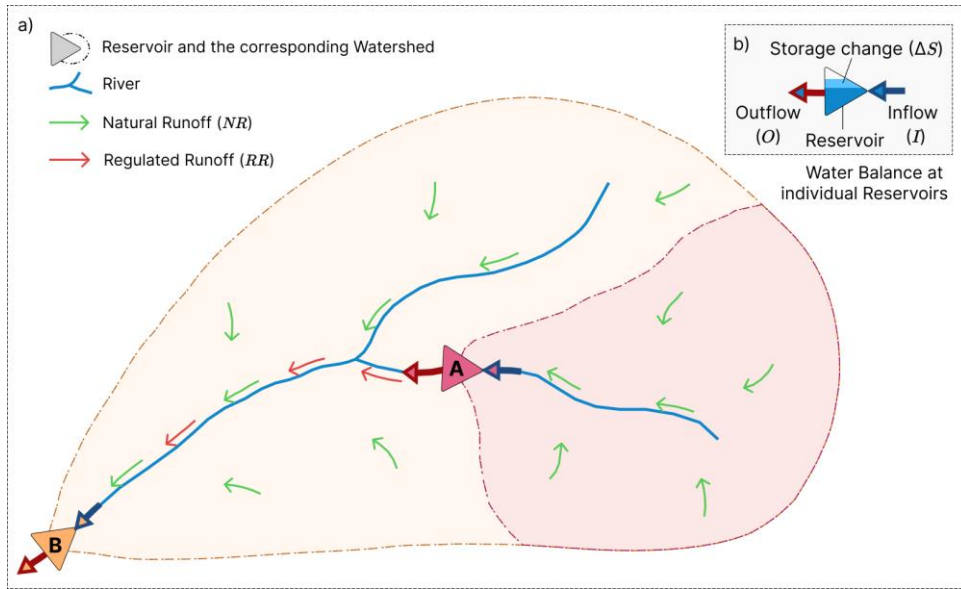


Figure 3: Conceptual schematic of the ResORR model. Panel (a) depicts the flow of surface runoff and streamflow, along with the contribution of the natural (green arrows) and regulated (red arrows along the stream) components, referred to in this paper as Natural Runoff (NR) and Regulated Runoff (RR) to the Inflow ( $I = NR + RR$ ) to a reservoir. Panel (b) describes the components of the water balance equation ( $O = I - \Delta S$ ) used at the reservoir to obtain the outflow from the reservoir, which is treated as the regulated component of the downstream streamflow.

As discussed above, the RR is defined as the component of inflow to a reservoir due to upstream reservoir releases. It is estimated as the sum of all Outflow (O) of the upstream reservoirs.

$$RR_i = \sum_j^N O_j \quad (2)$$

Where  $RR_i$  is the incoming Regulated Runoff to reservoir  $i$ ;  $O_j$  is the Outflow from the  $j^{th}$  upstream reservoir;  $N$  is the total number of upstream dams for reservoir  $i$ .

The NR is defined as the volume of water inflow to the reservoir due to surface runoff unaffected by any upstream reservoir operations., i.e., the generated surface runoff drains directly to the reservoir, without passing through any other reservoir. This surface runoff is generated in the part of the watershed which is not shared by any other upstream dams. For instance, in Figure 3, the orange and red shaded regions of the watershed will generate the NR for reservoirs B and A respectively. The NR for a reservoir can be estimated using the theoretical inflow into a reservoir if there were no upstream dams, which is referred to as the Theoretical Natural Runoff (TNR) in this paper. The Theoretical Natural Runoff (TNR) refers to the inflow to a reservoir if none of the upstream dams existed. The TNR can be calculated using the following equation –

$$TNR_i = NR_i + \sum_j^N NR_j \quad (3)$$

Where,  $TNR_i$  is the Theoretical Natural Runoff of reservoir  $i$ ;  $NR_i$  is the Natural Runoff to reservoir  $i$ ; and  $N$  is the total number of upstream dams of reservoir  $i$  along the same river network. For example, in the schematic in Figure 3, the TNR of reservoir A and B would be  $NR_A$  and  $NR_B + NR_A$  respectively.

Since the TNR represents streamflow into a reservoir in pristine conditions (without considering upstream reservoirs), it is analogous to the modeled inflow at reservoirs using traditional hydrologic models which do not take reservoir operations into account. The NR of any reservoir can be obtained by rearranging the terms of (3), and calculating the NR for reservoirs by iteratively moving downstream for each time-step. The NR for any reservoir can hence be obtained using the TNR of the reservoir, and the NR of the upstream reservoirs using the following equation –

$$NR_i = TNR_i - \sum_j^N NR_j \quad (4)$$

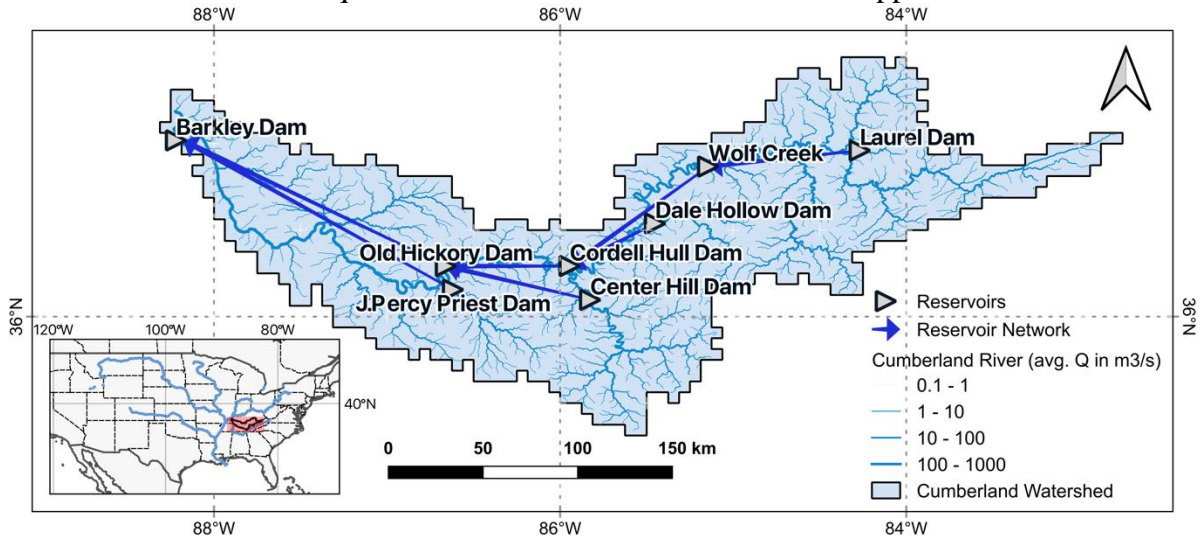
Using the estimated NR and RR components, the inflow to a reservoir under regulated conditions is then calculated using (1). Using the storage change of the reservoir, obtained either in-situ or using satellite estimates, the outflow can then be calculated using the water balance equation –

$$O = I - \Delta S \quad (5)$$

Where  $O$ ,  $I$  and  $\Delta S$  are the outflow, inflow and storage change of a reservoir respectively. In the current form of the mass balance equation of the reservoir fluxes, the evaporative losses are not considered. For semi-arid to arid parts of the world, such as the Western US, the Middle East, and Australia, evaporation from reservoirs can play an important role in reservoir water balance (Zhao et al. 2022). For the application ResORR over the Cumberland basin, which has a humid subtropical climate and is a relatively wet region. Here, the evaporative losses from reservoirs do not play a major role in the water balance and was hence safely ignored. For instance, the evaporation from the Wolf Creek reservoir is about only 1-2% of the total inflow to the reservoir annually.

329

These equations were solved for the reservoirs mapped in



330

331 Figure 2 by traversing down the network of reservoirs for each time-step. Since the TNR  
 332 is obtained by routing water through the watershed, the travel time of water between the reservoirs  
 333 is inherently considered in the subsequent calculations that depend on this routed hydrograph. The  
 334 proposed methodology is not a routing scheme, rather it operates on precomputed hydrographs  
 335 obtained by routing water through a watershed using traditional routing algorithms. The proposed  
 336 algorithm uses observational reservoir operations, either from in-situ or satellite platforms to adjust  
 337 the streamflow for regulation due to upstream reservoir operations in a post-processing fashion.

338

339 To assess the performance of the model, sensitivity to uncertainties in the model inputs,  
 340 and generally investigate the limitations of the model, various experiments were setup which are  
 341 discussed in section 4.1. To test the theoretical robustness of the proposed river regulation  
 342 algorithm as a mass conserving scheme, we set up a two inter-connected linear reservoir problem  
 343 where outflow is proportional to water storage and according to the elevation head available at the  
 344 outlet. Using this set up we generated regulated inflow that should theoretically happen at the  
 345 second reservoir (reservoir 2) based on storage and regulation effect of the upstream reservoir  
 346 (reservoir 1). Consequently, we tested the algorithm's ability to mimic the same regulated inflow  
 347 to reservoir 2 using storage and upstream unregulated inflow of reservoir 1 that would be available  
 348 in a globally scalable manner from satellite observations and modeling platforms such as RAT 3.0.  
 349 Our algorithm demonstrated perfect theoretical consistency as a mass conserving scheme. More  
 350 details on this theoretical robustness check of the ResORR algorithm are provided in the appendix  
 (section 7).

### 351 3.2. Reservoir network

352

353 The reservoir network represents the connectivity of the reservoirs in the model and is  
 354 represented by a directed tree data structure, with the nodes representing the reservoirs and the  
 355 links depicting their connectivity, while preserving the order of reservoirs. The model first  
 356 topologically sorts the reservoir network, to order them such that the water balance computations  
 357 of upstream reservoirs are performed before the subsequent downstream reservoir. At each time-  
 358 step, the model iterates over the topologically sorted reservoir network, and solves the series of  
 359 equations discussed in 3.1.

The reservoir network is generated using the location of reservoirs and the Global Dominant River Tracing (DRT) dataset (Wu et al., 2011). Since the river-regulation model is designed as an add-on to the RAT framework, the script to generate the reservoir network can use the inputs and intermediary outputs of RAT to generate the reservoir network.

## 4. Experiments and Results

### 4.1. River regulation experiment setups using in-situ data

The ResORR algorithm is fully described by equations (1)-(5), which uses estimates of streamflow under pristine conditions from a hydrological model. However, the uncertainties in the estimations of hydrological model may propagate as uncertainty in the river-regulation model. Experiments were performed to isolate the performance of the core of the algorithm, its ability to partition the inflow between the natural and regulated components using in-situ observations in place of hydrological model and satellite estimates. By reducing uncertainties in certain parts of the algorithm, the performance of the individual components could be investigated, shedding light on the sensitivity of the algorithm components to the input data accuracy. Moreover, the observed in-situ  $\Delta S$  was used in these experiments to gauge the baseline performance of ResORR using best available reservoir operations data, avoiding the higher uncertainties normally associated with satellite estimates of storage change.

To investigate the strengths and weaknesses of ResORR, especially in terms of scalability, the experiment designs were iteratively modified and updated in order from E1 to E4 over the period of 2015-2019. Details about the experiment designs and the rationale behind the experiments are summarized in Table 1.

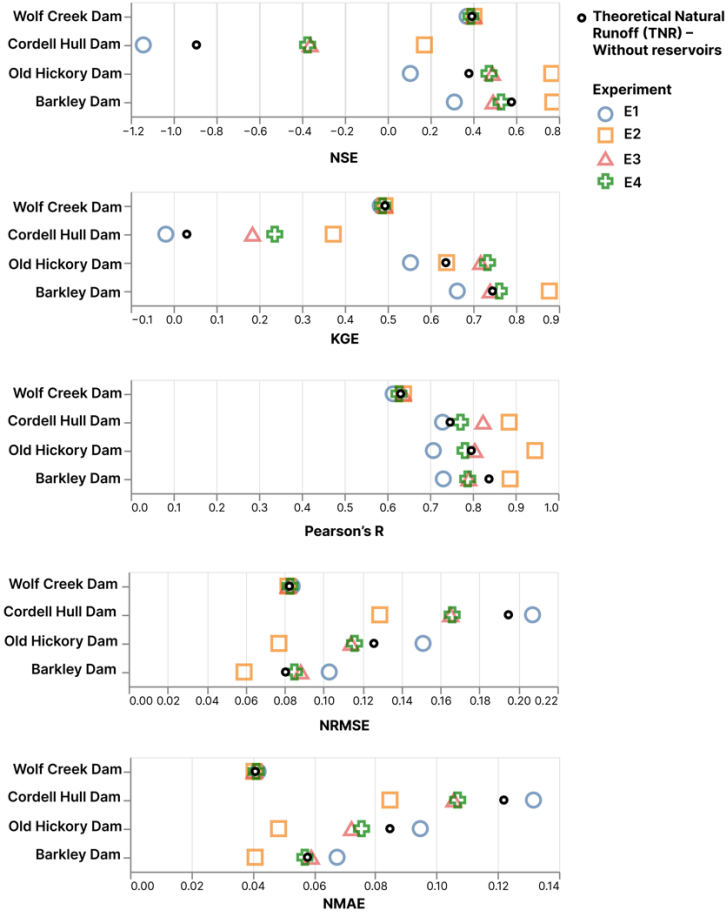
Table 1: Summary of the experiments performed on the river regulation model along with the corresponding symbols used in the performance comparison plot (Figure 4).

Exp.	In-situ data used	Description	Rationale
E1 	$\Delta S$	In-situ $\Delta S$ was used in eqn. (5) to estimate O. VIC hydrologic model was not calibrated for estimating natural inflow.	Uncertainties in satellite estimates of $\Delta S$ are minimized in this experiment.
E2 	O	Observed O was used in eqn. (3) to estimate RR.	Uncertainties in otherwise estimated O, due to uncertainties in modeled I are minimized. The RR obtained as such would reflect the “theoretically” best estimate of incoming regulated streamflow.
E3 	I, $\Delta S$	Observed I was used in eqn. (4) only at the most upstream dam, where $NR = TNR = I$ . In-situ $\Delta S$ was used in (5) to estimate O.	For upstream-most reservoirs all the incoming streamflow would be due to natural runoff, hence, by using the observed I, the uncertainties due to modeled I are minimized. The RR in this

1  
2  
3  
4  
5  
6  
7  
8  
9  
10  
11  
12  
13  
14  
15  
16  
17  
18  
19  
20  
21  
22  
23  
24  
25  
26  
27  
28  
29  
30  
31  
32  
33  
34  
35  
36  
37  
38  
39  
40  
41  
42  
43  
44  
45  
46  
47  
48  
49  
50  
51  
52  
53  
54  
55  
56  
57  
58  
59  
60  
61  
62  
63  
64  
65

			case would reflect the “theoretical best estimate” of the downstream regulated streamflow.
E4 	$\Delta S$	In-situ $\Delta S$ resampled to a 16-day frequency was used in eq (5) to estimate O. The VIC hydrological model, forced with satellite data, was calibrated at upstream most dams of Center Hill Dam, Dale Hollow Dam, and Laurel Dam.	The modeled inflow to the upstream most dams were calibrated using the observed inflow, essentially, minimizing the uncertainties at the upstream boundary of the reservoir network. This represents the ResORR in its globally scalable form under the scenario of perfect $\Delta S$ at observational frequency of satellites. The resampling to 16-day frequency was done to simulate the observational frequency of the satellites used later in this study. ResORR can adapt to any observational frequency of satellite-based storage estimates.

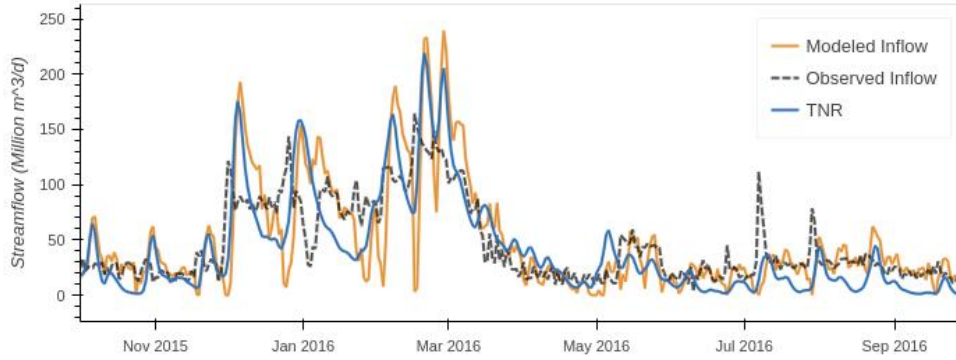
The regulated inflows obtained at the 4 dams, which have at least one upstream dam were compared against the observed inflow at those same dams. The comparison statistics measuring the performance of the river regulation model against observed inflow data are summarized in Figure 4. To understand how the river regulation algorithm is performing under various input scenarios and assumptions, one should compare the relative position of the symbols for each dam along the horizontal axis only. The TNR, obtained from the VIC hydrological model are denoted using grey and black circles, corresponding to the streamflow modeled using default parameter values and calibrated parameters. Formulation of performance metrics are provided in Appendix (section 7).



391  
 392  
 393  
 394  
 395  
 396  
 397  
 398  
 399  
 400  
 401  
 402  
 403  
 404  
 405  
 406  
 407  
 408  
 409  
 410  
 411  
 Figure 4: River regulation model performance for E\* experiments using in-situ reservoir dynamics data.

394 394 Compared to the uncalibrated VIC streamflow estimates, the performance of the river  
 395 395 regulation model in the E1 experiment in improving the accuracy of regulated inflow seems to be  
 396 396 reduced. In other words, ResORR using in-situ  $\Delta S$ , but with uncalibrated VIC flow at upstream  
 397 397 most location does not improve the skill in predicted regulated inflow at downstream dam  
 398 398 locations. However, on taking a closer look at the hydrographs comparing modeled inflow, TNR  
 399 399 and observed inflow in Figure 5, it is apparent that the variability in the observed inflow, which is  
 400 400 regulated inflow, is more closely replicated by the variability in the modeled inflow than the TNR.  
 401 401 This likely suggests that even though the overall performance of ResORR gets reduced as a  
 402 402 regulated streamflow predictor, the signature of human regulation is still captured well.

403 403 While analyzing the observed inflow hydrographs of two consecutive dams (Cordell Hull  
 404 404 and Old Hickory dams) in Figure 6, a closer relationship between the downstream inflow and  
 405 405 upstream outflow can be noted. It is clear that the upstream outflow plays a dominant role in  
 406 406 dictating the downstream and regulated inflow at the next downstream dam as would be normally  
 407 407 expected in the event of no lateral flow diversion. This relationship is further explored in the E2  
 408 408 experiment, where the daily in-situ outflow is used to calculate the RR to the downstream dam.  
 409 409 Overall, the results improve across the board in the E2 experiment, underlining the role of upstream  
 410 410 reservoir releases in predicting the downstream regulated streamflow. The E2 experiment also  
 411 411 stresses the importance of having high accuracy estimates of reservoir storage data.



412  
413  
414  
415  
416  
417  
418  
419  
420  
421  
422  
423  
424  
425  
426  
427  
428  
429  
430  
431  
432  
433  
434  
435  
436  
437  
438  
439  
440  
441  
442  
443  
444  
445  
446  
447  
448  
449  
450  
451  
452  
453  
454  
455  
456  
457  
458  
459  
460  
461  
462  
463  
464  
465

Figure 5: Hydrographs comparing the Modeled, Observed and TNR at Old Hickory Dam, which is the second most downstream dam in the network. The observed inflow is regulated inflow.

In the E3 experiment, the observed inflow to the upstream most dams was used as the NR. In most cases, the performance of the streamflow predictions still improved when adjusted for upstream regulation, as compared to the TNR. While this experiment suggests that if the accuracy of inflow estimates at the upstream most boundary conditions are accurate, that can improve the regulated streamflow estimates along that downstream network as well. Following this, the final E4 experiment, representative of the performance of the proposed and scalable river regulation model under accurate  $\Delta S$  was performed. Here the VIC hydrological model was calibrated using the observed inflow at the upstream most dams. The result of this experiment shows overall improvement for nearly all the reservoirs. These results indicate that using in-situ reservoir dynamics, specifically storage change, and inflow hydrograph modeled without considering reservoirs (TNR) can be used to improve the performance of downstream streamflow estimates.

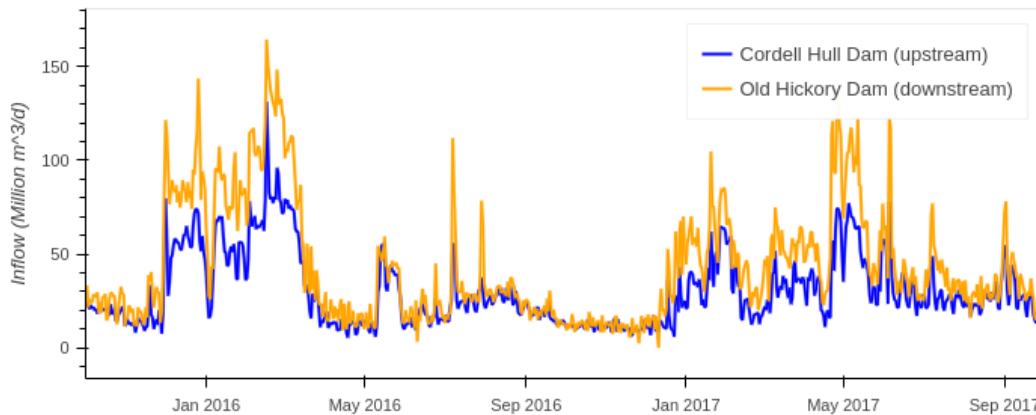


Figure 6: Observed inflows at two consecutive dams. The upstream Cordell Hull Dam drains into the downstream Old Hickory Dam, with the effect of upstream reservoir dynamics.

Moreover, the experiment results also shed light on the relationship between the model performance and the number of upstream dams. For instance, taking the case of the Wolf Creek dam (7.4 km<sup>3</sup> storage capacity), which only has one upstream dam (Laurel Dam, 0.5 km<sup>3</sup> storage capacity), the performance of the model does not improve as significantly as compared to the TNR. On the other hand, Cordell Hull Dam (run-of-the-river) is highly regulated and has two upstream dams, the Dale Hollow dam (2.1 km<sup>3</sup>) and the Wolf Creek dam, and the performance of the streamflow estimates improves significantly by almost 50% across all the dams in the basin.

Overall, the results show that considering the effect of upstream regulation improves the performance of the streamflow estimates at the downstream dams.

## 4.2. River regulation using satellite estimates of reservoir storage change

Now that E4 results established robustness of the proposed river regulation algorithm, we explore how well ResORR fares with satellite-derived  $\Delta S$  that will have higher uncertainty. The inundation area of the reservoirs were obtained using the Landsat-8 and Sentinel-1 satellite data from June 2018 to October 2019, using the TMS-OS algorithm described by Das et al., (2022). The storage change of the reservoirs were then obtained using these surface area estimates and in-situ Area-Elevation Curve (AEC), using the following equation –

$$\Delta S_t = \frac{A_t + A_{t-1}}{2} \times (h_t - h_{t-1}) \quad (6)$$

Here the  $\Delta S$  in equation 6 is the total volumetric storage change,  $A$  is the inundation area, and  $h$  is the water level height corresponding to the inundation area, obtained using the AEC relationship. The date of satellite observation is denoted by  $t$ , with  $t - 1$  referring to the last satellite observation. For instance, since Landsat-8 has a revisit period of 16 days, the estimated storage change would refer to the volumetric storage change within those 16 days. These storage change estimates were transformed to daily values by linearly distributing the volumetric change over 16 days. Based on the findings of the previous section, the VIC hydrological model was calibrated at the upstream most dams, like the E4 experiment. The modeled inflow as such and the streamflow estimates from VIC were compared against the observed in-situ inflow. The results are summarized in Figure 7.

Similar to the results in the previous section, for the Cordell Hull and Old Hickory, both run-of-the-river dams having upstream dams with large storage capacities, ResORR performance increases significantly across all metrics. For the Wolf Creek dam, adjusting for the upstream Laurel Dam's operations, ResORR performance does not increase as drastically, which can be explained due to the relatively smaller size of the upstream Laurel Dam. In contrast, the performance increases the most for the Cordell Hull Dam, which is preceded by two large dams, Wolf Creek Dam and Dale Hollow dam. The improvement in performance gradually reduces downstream with marginal improvement for the downstream most Barkley Dam. This can be explained by the run-of-the-river nature of the upstream dams, the storage change dynamics of which can be difficult to quantify using satellite observations. Overall, the results suggest that river regulation due to dams can be characterized by the proposed ResORR algorithm using satellite estimates of reservoir storage dynamics. Adjusting for flow regulation due to upstream reservoir storage change improves the overall inflow predictions in a regulated basin.

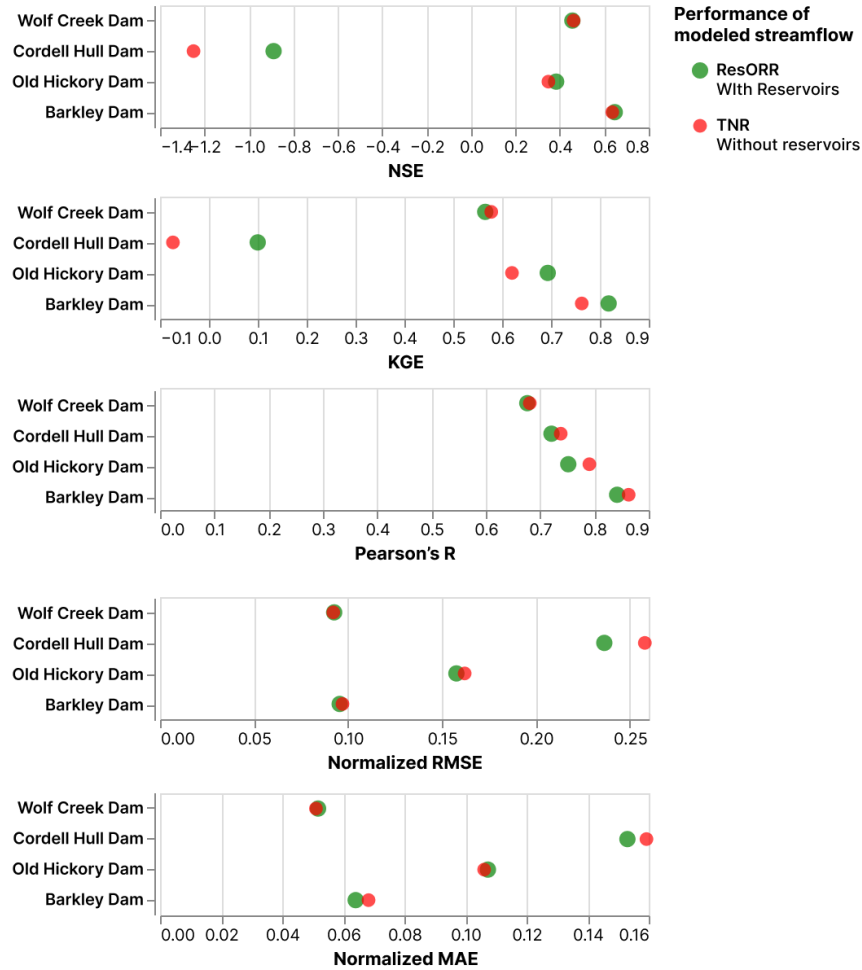


Figure 7: ResORR model performance using satellite derived reservoir storage change.

## 5. Conclusions and Discussion

Rivers of the 21<sup>st</sup> century are marked with numerous reservoirs, which store, and release water based on their primary objectives, playing a vital role in providing food, water, and energy security. However, such reservoir operations can alter the natural streamflow patterns, reducing the water availability downstream by storing water during high flows, and *vice versa*. In this study, we developed and tested a scalable river regulation model, ResORR, to predict the regulation of streamflow due to upstream reservoir operations. Overall, we find that adjusting for upstream reservoir operations via storage change improves the accuracy of downstream streamflow predictions. The theoretical basis of the ResORR model was tested using in-situ data in the heavily regulated Cumberland basin. The results stress the importance of having high accuracy estimates of both the storage change and the hydrological model. Moreover, we find that if the hydrological model can be calibrated for boundary conditions of the reservoir network, *i.e.*, at the upstream most dams, significant improvement can be achieved in predicting regulated inflow at all the downstream dam locations.

Currently, the reservoir network is automatically generated using the dam locations and the DRT flow directions, and hence, any inter- or intra-basin diversions between reservoirs or lateral

1  
2  
3  
4 487 diversions cannot yet be modeled. The regulation caused by reservoirs is also determined by its  
5 488 storage capacity, and in a case where a small reservoir drains into a larger reservoir, the algorithm  
6 489 adds little value to the streamflow predictions. Moreover, if the storage change of the upstream  
7 490 reservoir is relatively low, the performance improvement of regulated streamflow estimation  
8 491 downstream can be limited. Such a case was experienced in a case-study of the devastating flood  
9 492 due to extreme precipitation in the state of Kerala, India, in 2018. Due to high precipitation leading  
10 493 up to the main extreme precipitation event, the reservoirs were already at full supply level. All the  
11 494 incoming inflow due to the extreme precipitation event had to be released by the upstream  
12 495 reservoir, with little to no storage change. Even with these limitations, the ResORR algorithm can  
13 496 play an important role in quantifying the regulation of river flow due to reservoirs in changing the  
14 497 world's river systems.

15  
16  
17  
18 498 With advancements in satellite observations-based reservoir dynamics tracking, especially  
19 499 the RAT 3.0, which has democratized access to reservoir operations information, it is now possible  
20 500 to easily track the operations of reservoirs globally. Building on top of the RAT framework, the  
21 501 proposed river regulation algorithm ResORR would also be able to characterize the regulation of  
22 502 river flow using only satellite-tracked reservoir states at the global scale. The algorithm was  
23 503 developed over the Cumberland basin which is in a humid region. The evaporative losses from the  
24 504 reservoirs therefore play a relatively minor role compared to the inflow into the reservoir due to  
25 505 surface runoff. Hence, the evaporative losses were not considered while calculating the outflow.  
26 506 However, the evaporative losses play an important role in arid regions. For application over such  
27 507 regions, the evaporation from the reservoirs can be included in the water mass balance of the  
28 508 reservoirs in eq. (5). The ResORR software architecture is also designed to work seamlessly within  
29 509 the RAT framework, i.e., it can run entirely using the RAT model outputs and intermediary files.  
30 510 With this river regulation tool, the RAT framework will be able to not only infer reservoir  
31 511 dynamics, but also quantify the regulation of streamflow caused by the upstream reservoir  
32 512 operations. We can expect ResORR to soon become a truly scalable algorithm based on the  
33 513 globally available reservoir storage change data of unprecedented accuracy from the Surface Water  
34 514 and Ocean Topography mission.

35  
36  
37  
38 515 **Acknowledgements:** This study was supported by NASA Applied Science grants from the Water  
39 516 Resources Program (80NSSC22K0918) and the Capacity Building Program (80NSSC23K0184).  
40 517 All co-authors from the University of Washington, co-author Lee from University of Houston, and  
41 518 co-author Andreadis from University of Massachusetts were supported by both these programs.  
42 519

43  
44  
45  
46 520 **Author role:**

47 521 Research implementation: Pritam Das

48 522 Research design, data, and manuscript writing: Pritam Das and Faisal Hossain

49 523 Data, software and manuscript editing: Sanchit Minocha, George Darkwah and Sarath Suresh

50 524 Data and manuscript editing: Hyongki Lee and Konstantinos Andreadis

51 525 Research design and manuscript editing: Miguel Laverde-Barajas and Perry Oddo  
52  
53  
54  
55  
56  
57  
58  
59  
60  
61  
62  
63  
64  
65

## 6. References

- Ahmad, S. K., Hossain, F., Holtgrieve, G. W., Pavelsky, T., & Galelli, S. (2021). Predicting the Likely Thermal Impact of Current and Future Dams Around the World. *Earth's Future*, 9(10), e2020EF001916. <https://doi.org/10.1029/2020EF001916>
- Alcamo, J., Döll, P., Henrichs, T., Kaspar, F., Lehner, B., Rösch, T., & Siebert, S. (2003). Development and testing of the WaterGAP 2 global model of water use and availability. *Hydrological Sciences Journal*, 48(3), 317–337. <https://doi.org/10.1623/hysj.48.3.317.45290>
- Biancamaria, S., Lettenmaier, D. P., & Pavelsky, T. M. (2016). The SWOT Mission and Its Capabilities for Land Hydrology. *Surveys in Geophysics*, 37(2), 307–337. <https://doi.org/10.1007/s10712-015-9346-y>
- Biemans, H., Haddeland, I., Kabat, P., Ludwig, F., Hutjes, R. W. A., Heinke, J., von Bloh, W., & Gerten, D. (2011). Impact of reservoirs on river discharge and irrigation water supply during the 20th century. *Water Resources Research*, 47(3). <https://doi.org/10.1029/2009WR008929>
- Biswas, N. K., & Hossain, F. (2022). A Multidecadal Analysis of Reservoir Storage Change in Developing Regions. *Journal of Hydrometeorology*, 23(1), 71–85. <https://doi.org/10.1175/JHM-D-21-0053.1>
- Biswas, N. K., Hossain, F., Bonnema, M., Lee, H., & Chishtie, F. (2021). Towards a global Reservoir Assessment Tool for predicting hydrologic impacts and operating patterns of existing and planned reservoirs. *Environmental Modelling & Software*, 140, 105043. <https://doi.org/10.1016/j.envsoft.2021.105043>

1  
2  
3  
4  
5  
6  
7  
8  
9  
10  
11  
12  
13  
14  
15  
16  
17  
18  
19  
20  
21  
22  
23  
24  
25  
26  
27  
28  
29  
30  
31  
32  
33  
34  
35  
36  
37  
38  
39  
40  
41  
42  
43  
44  
45  
46  
47  
48  
49  
50  
51  
52  
53  
54  
55  
56  
57  
58  
59  
60  
61  
62  
63  
64  
65

548 Bonnema, M., & Hossain, F. (2017). Inferring reservoir operating patterns across the Mekong  
549 Basin using only space observations. *Water Resources Research*, 53(5), 3791–3810.  
550 <https://doi.org/10.1002/2016WR019978>

551 Bonnet, M., Witt, A., Steart, K., Hadjerioua, B., & Mobley, M. (2015). *The Economic Benefits of*  
552 *Multipurpose Reservoirs in the United States-Federal Hydropower Fleet*.  
553 <https://doi.org/10.13140/RG.2.2.15894.14400>

554 Caissie, D. (2006). The thermal regime of rivers: A review. *Freshwater Biology*, 51(8), 1389–  
555 1406. <https://doi.org/10.1111/j.1365-2427.2006.01597.x>

556 Cheng, Y., Nijssen, B., Holtgrieve, G. W., & Olden, J. D. (2022). Modeling the freshwater  
557 ecological response to changes in flow and thermal regimes influenced by reservoir  
558 dynamics. *Journal of Hydrology*, 608, 127591.  
559 <https://doi.org/10.1016/j.jhydrol.2022.127591>

560 Cheng, Y., Voisin, N., Yearsley, J. R., & Nijssen, B. (2020). Reservoirs Modify River Thermal  
561 Regime Sensitivity to Climate Change: A Case Study in the Southeastern United States.  
562 *Water Resources Research*, 56(6), e2019WR025784.  
563 <https://doi.org/10.1029/2019WR025784>

564 Cooley, S. W., Ryan, J. C., & Smith, L. C. (2021). Human alteration of global surface water  
565 storage variability. *Nature*, 591(7848), Article 7848. [https://doi.org/10.1038/s41586-](https://doi.org/10.1038/s41586-021-03262-3)  
566 [021-03262-3](https://doi.org/10.1038/s41586-021-03262-3)

567 Das, P., Hossain, F., Khan, S., Biswas, N. K., Lee, H., Piman, T., Meechaiya, C., Ghimire, U., &  
568 Hosen, K. (2022). Reservoir Assessment Tool 2.0: Stakeholder driven improvements to

1  
2  
3  
4 569 satellite remote sensing based reservoir monitoring. *Environmental Modelling &*  
5  
6  
7 570 *Software*, 157(105533). <https://doi.org/10.1016/j.envsoft.2022.105533>  
8  
9  
10 571 Dong, N., Yang, M., Wei, J., Arnault, J., Laux, P., Xu, S., Wang, H., Yu, Z., & Kunstmann, H. (2023).  
11  
12 572 Toward Improved Parameterizations of Reservoir Operation in Ungauged Basins: A  
13  
14  
15 573 Synergistic Framework Coupling Satellite Remote Sensing, Hydrologic Modeling, and  
16  
17 574 Conceptual Operation Schemes. *Water Resources Research*, 59(3), e2022WR033026.  
18  
19  
20 575 <https://doi.org/10.1029/2022WR033026>  
21  
22 576 Dunn, F. E., Darby, S. E., Nicholls, R. J., Cohen, S., Zarfl, C., & Fekete, B. M. (2019). Projections of  
23  
24  
25 577 declining fluvial sediment delivery to major deltas worldwide in response to climate  
26  
27  
28 578 change and anthropogenic stress. *Environmental Research Letters*, 14(8), 084034.  
29  
30 579 <https://doi.org/10.1088/1748-9326/ab304e>  
31  
32  
33 580 Earth Resources Observation And Science (EROS) Center. (2017). *Shuttle Radar Topography*  
34  
35 581 *Mission (SRTM) 1 Arc-Second Global* [Tiff]. U.S. Geological Survey.  
36  
37  
38 582 <https://doi.org/10.5066/F7PR7TFT>  
39  
40  
41 583 Eldardiry, H., & Hossain, F. (2021). A blueprint for adapting high Aswan dam operation in Egypt  
42  
43 584 to challenges of filling and operation of the Grand Ethiopian Renaissance dam. *Journal*  
44  
45  
46 585 *of Hydrology*, 598, 125708. <https://doi.org/10.1016/j.jhydrol.2020.125708>  
47  
48  
49 586 Gao, H., Birkett, C., & Lettenmaier, D. P. (2012). Global monitoring of large reservoir storage  
50  
51 587 from satellite remote sensing. *Water Resources Research*, 48(9), 2012WR012063.  
52  
53  
54 588 <https://doi.org/10.1029/2012WR012063>  
55  
56 589 Gupta, H. V., Kling, H., Yilmaz, K. K., & Martinez, G. F. (2009). Decomposition of the mean  
57  
58  
59 590 squared error and NSE performance criteria: Implications for improving hydrological  
60  
61  
62  
63  
64  
65

1  
2  
3  
4 591 modelling. *Journal of Hydrology*, 377(1–2), 80–91.  
5  
6  
7 592 <https://doi.org/10.1016/j.jhydrol.2009.08.003>  
8  
9  
10 593 Haddeland, I., Skaugen, T., & Lettenmaier, D. P. (2006). Anthropogenic impacts on continental  
11  
12 594 surface water fluxes. *Geophysical Research Letters*, 33(8), L08406.  
13  
14  
15 595 <https://doi.org/10.1029/2006GL026047>  
16  
17 596 Han, Z., Long, D., Huang, Q., Li, X., Zhao, F., & Wang, J. (2020). Improving Reservoir Outflow  
18  
19  
20 597 Estimation for Ungauged Basins Using Satellite Observations and a Hydrological Model.  
21  
22 598 *Water Resources Research*, 56(9), e2020WR027590.  
23  
24  
25 599 <https://doi.org/10.1029/2020WR027590>  
26  
27  
28 600 Hanasaki, N., Kanae, S., & Oki, T. (2006). A reservoir operation scheme for global river routing  
29  
30 601 models. *Journal of Hydrology*, 327(1–2), 22–41.  
31  
32  
33 602 <https://doi.org/10.1016/j.jhydrol.2005.11.011>  
34  
35  
36 603 Hanasaki, N., Yoshikawa, S., Pokhrel, Y., & Kanae, S. (2018). A global hydrological simulation to  
37  
38 604 specify the sources of water used by humans. *Hydrology and Earth System Sciences*,  
39  
40 605 22(1), 789–817. <https://doi.org/10.5194/hess-22-789-2018>  
41  
42  
43 606 Hersbach, H., Bell, B., Berrisford, P., Hirahara, S., Horányi, A., Muñoz-Sabater, J., Nicolas, J.,  
44  
45 607 Peubey, C., Radu, R., Schepers, D., Simmons, A., Soci, C., Abdalla, S., Abellan, X.,  
46  
47  
48 608 Balsamo, G., Bechtold, P., Biavati, G., Bidlot, J., Bonavita, M., ... Thépaut, J. (2020). The  
49  
50  
51 609 ERA5 global reanalysis. *Quarterly Journal of the Royal Meteorological Society*, 146(730),  
52  
53 610 1999–2049. <https://doi.org/10.1002/qj.3803>  
54  
55  
56 611 Hossain, F., Sikder, S., Biswas, N., Bonnema, M., Lee, H., Luong, N. D., Hiep, N. H., Du Duong, B.,  
57  
58 612 & Long, D. (2017). Predicting Water Availability of the Regulated Mekong River Basin  
59  
60  
61  
62  
63  
64  
65

1  
2  
3  
4  
5  
6  
7  
8  
9  
10  
11  
12  
13  
14  
15  
16  
17  
18  
19  
20  
21  
22  
23  
24  
25  
26  
27  
28  
29  
30  
31  
32  
33  
34  
35  
36  
37  
38  
39  
40  
41  
42  
43  
44  
45  
46  
47  
48  
49  
50  
51  
52  
53  
54  
55  
56  
57  
58  
59  
60  
61  
62  
63  
64  
65

613 Using Satellite Observations and a Physical Model. *Asian Journal of Water, Environment*  
614 *and Pollution*, 14(3), 39–48. <https://doi.org/10.3233/AJW-170024>

615 Knobon, W. J. M., Freer, J. E., & Woods, R. A. (2019). *Technical note: Inherent benchmark or*  
616 *not? Comparing Nash-Sutcliffe and Kling-Gupta efficiency scores* [Preprint]. Catchment  
617 hydrology/Modelling approaches. <https://doi.org/10.5194/hess-2019-327>

618 Lee, H., Durand, M., Jung, H. C., Alsdorf, D., Shum, C. K., & Sheng, Y. (2010). Characterization of  
619 surface water storage changes in Arctic lakes using simulated SWOT measurements.  
620 *International Journal of Remote Sensing*, 31(14), 3931–3953.  
621 <https://doi.org/10.1080/01431161.2010.483494>

622 Li, S., Xu, Y. J., & Ni, M. (2021). Changes in sediment, nutrients and major ions in the world  
623 largest reservoir: Effects of damming and reservoir operation. *Journal of Cleaner*  
624 *Production*, 318, 128601. <https://doi.org/10.1016/j.jclepro.2021.128601>

625 Liang, X., Lettenmaier, D. P., Wood, E. F., & Burges, S. J. (1994). A simple hydrologically based  
626 model of land surface water and energy fluxes for general circulation models. *Journal of*  
627 *Geophysical Research: Atmospheres*, 99(D7), 14415–14428.  
628 <https://doi.org/10.1029/94JD00483>

629 Lohmann, D., Raschke, E., Nijssen, B., & Lettenmaier, D. P. (1998). Regional scale hydrology: I.  
630 Formulation of the VIC-2L model coupled to a routing model. *Hydrological Sciences*  
631 *Journal*, 43(1), 131–141. <https://doi.org/10.1080/02626669809492107>

632 Marcaida, M., Farhat, Y., Muth, E.-N., Cheythyrit, C., Hok, L., Holtgrieve, G., Hossain, F.,  
633 Neumann, R., & Kim, S.-H. (2021). A spatio-temporal analysis of rice production in Tonle

1  
2  
3  
4  
5  
6  
7  
8  
9  
10  
11  
12  
13  
14  
15  
16  
17  
18  
19  
20  
21  
22  
23  
24  
25  
26  
27  
28  
29  
30  
31  
32  
33  
34  
35  
36  
37  
38  
39  
40  
41  
42  
43  
44  
45  
46  
47  
48  
49  
50  
51  
52  
53  
54  
55  
56  
57  
58  
59  
60  
61  
62  
63  
64  
65

634 Sap floodplains in response to changing hydrology and climate. *Agricultural Water*  
635 *Management*, 258, 107183. <https://doi.org/10.1016/j.agwat.2021.107183>

636 Minocha, S., Hossain, F., Das, P., Suresh, S., Khan, S., Darkwah, G., Lee, H., Galelli, S., Andreadis,  
637 K., & Oddo, P. (2023). Reservoir Assessment Tool Version 3.0: A Scalable and User-  
638 Friendly Software Platform to Mobilize the Global Water Management Community.  
639 *Geoscientific Model Development Discussions*, 2023, 1–23.  
640 <https://doi.org/10.5194/gmd-2023-130>

641 Nash, J. E., & Sutcliffe, J. V. (1970). River flow forecasting through conceptual models part I — A  
642 discussion of principles. *Journal of Hydrology*, 10(3), 282–290.  
643 [https://doi.org/10.1016/0022-1694\(70\)90255-6](https://doi.org/10.1016/0022-1694(70)90255-6)

644 Neel, J. K., & Allen, W. R. (1964). The mussel fauna of the upper Cumberland Basin before its  
645 impoundment. *Malacologia*, 1(3), 427–459.

646 Okeowo, M. A., Lee, H., Hossain, F., & Getirana, A. (2017). Automated Generation of Lakes and  
647 Reservoirs Water Elevation Changes From Satellite Radar Altimetry. *IEEE Journal of*  
648 *Selected Topics in Applied Earth Observations and Remote Sensing*, 10(8), 3465–3481.  
649 <https://doi.org/10.1109/JSTARS.2017.2684081>

650 Pokhrel, Y., Shin, S., Lin, Z., Yamazaki, D., & Qi, J. (2018). Potential Disruption of Flood Dynamics  
651 in the Lower Mekong River Basin Due to Upstream Flow Regulation. *Scientific Reports*,  
652 8(1), Article 1. <https://doi.org/10.1038/s41598-018-35823-4>

653 Robinson, J. A. (2019). *Estimated use of water in the Cumberland River watershed in 2010 and*  
654 *projections of public-supply water use to 2040* (Report 2018–5130; Scientific

1  
2  
3  
4 655 Investigations Report, p. 74). USGS Publications Warehouse.  
5  
6  
7 656 <https://doi.org/10.3133/sir20185130>  
8  
9  
10 657 Steyaert, J. C., Condon, L. E., W. D. Turner, S., & Voisin, N. (2022). ResOpsUS, a dataset of  
11  
12 658 historical reservoir operations in the contiguous United States. *Scientific Data*, 9(1),  
13  
14 659 Article 1. <https://doi.org/10.1038/s41597-022-01134-7>  
15  
16  
17 660 Suresh, S., Hossain, F., Minocha, S., Das, P., Khan, S., Lee, H., Andreadis, K., & Oddo, P. (2024).  
18  
19  
20 661 Satellite-based Tracking of Reservoir Operations for Flood Management during the 2018  
21  
22 662 Extreme Weather Event in Kerala, India. *Remote Sensing of Environment*, 1–34.  
23  
24  
25 663 Tippit, R. N., Brown, J. K., Sharber, J. F., & Miller, A. C. (1995). Modifying Cumberland River  
26  
27 664 system reservoir operations to improve mussel habitat. *Conservation and Management*  
28  
29 665 *of Freshwater Mussels II: Initiatives for the Future. Proceedings of a UMRCC Symposium*,  
30  
31 666 229–235.  
32  
33  
34  
35 667 USACE. (n.d.). *WM Data Dissemination*. Retrieved October 15, 2023, from  
36  
37 668 <https://water.usace.army.mil/a2w/f?p=100:1:::##>  
38  
39  
40 669 Vanderkelen, I., Gharari, S., Mizukami, N., Clark, M. P., Lawrence, D. M., Swenson, S., Pokhrel,  
41  
42 670 Y., Hanasaki, N., van Griensven, A., & Thiery, W. (2022). Evaluating a reservoir  
43  
44 671 parametrization in the vector-based global routing model mizuRoute (v2.0.1) for Earth  
45  
46 672 system model coupling. *Geoscientific Model Development*, 15(10), 4163–4192.  
47  
48 673 <https://doi.org/10.5194/gmd-15-4163-2022>  
49  
50  
51 674 Vu, D. T., Dang, T. D., Galelli, S., & Hossain, F. (2021). *Satellite observations reveal thirteen years*  
52  
53 675 *of reservoir filling strategies, operating rules, and hydrological alterations in the Upper*  
54  
55 676 *Mekong River Basin* [Preprint]. *Hydrology*. <https://doi.org/10.1002/essoar.10507302.1>  
56  
57  
58  
59  
60  
61  
62  
63  
64  
65

1  
2  
3  
4 677 Wada, Y., Bierkens, M. F. P., de Roo, A., Dirmeyer, P. A., Famiglietti, J. S., Hanasaki, N., Konar,  
5  
6  
7 678 M., Liu, J., Müller Schmied, H., Oki, T., Pokhrel, Y., Sivapalan, M., Troy, T. J., van Dijk, A. I.  
8  
9  
10 679 J. M., van Emmerik, T., Van Huijgevoort, M. H. J., Van Lanen, H. A. J., Vörösmarty, C. J.,  
11  
12 680 Wanders, N., & Wheeler, H. (2017). Human–water interface in hydrological modelling:  
13  
14  
15 681 Current status and future directions. *Hydrology and Earth System Sciences*, 21(8), 4169–  
16  
17 682 4193. <https://doi.org/10.5194/hess-21-4169-2017>  
18  
19  
20 683 Wilson, C. B., & Clark, H. W. (1914). *The mussels of the Cumberland River and its tributaries*  
21  
22 684 (Issue 781). US Government Printing Office.  
23  
24  
25 685 Wissler, D., & Fekete, B. M. (2009). *Reconstructing 20th century global hydrography*.  
26  
27  
28 686 Wu, H., Kimball, J. S., Mantua, N., & Stanford, J. (2011). Automated upscaling of river networks  
29  
30 687 for macroscale hydrological modeling: UPSCALING OF GLOBAL RIVER NETWORKS. *Water*  
31  
32  
33 688 *Resources Research*, 47(3). <https://doi.org/10.1029/2009WR008871>  
34  
35  
36 689 Yoon, Y., & Beighley, E. (2015). Simulating streamflow on regulated rivers using characteristic  
37  
38 690 reservoir storage patterns derived from synthetic remote sensing data. *Hydrological*  
39  
40  
41 691 *Processes*, 29(8), 2014–2026. <https://doi.org/10.1002/hyp.10342>  
42  
43  
44 692 Yoon, Y., Beighley, E., Lee, H., Pavelsky, T., & Allen, G. (2016). Estimating Flood Discharges in  
45  
46 693 Reservoir-Regulated River Basins by Integrating Synthetic SWOT Satellite Observations  
47  
48 694 and Hydrologic Modeling. *Journal of Hydrologic Engineering*, 21(4), 05015030.  
49  
50  
51 695 [https://doi.org/10.1061/\(ASCE\)HE.1943-5584.0001320](https://doi.org/10.1061/(ASCE)HE.1943-5584.0001320)  
52  
53  
54 696 Zhao, G., Li, Y., Zhou, L., & Gao, H. (2022). Evaporative water loss of 1.42 million global lakes.  
55  
56 697 *Nature Communications*, 13(1), 3686. <https://doi.org/10.1038/s41467-022-31125-6>  
57  
58  
59  
60  
61  
62  
63  
64  
65

1  
2  
3  
4  
5  
6  
7  
8  
9  
10  
11  
12  
13  
14  
15  
16  
17  
18  
19  
20  
21  
22  
23  
24  
25  
26  
27  
28  
29  
30  
31  
32  
33  
34  
35  
36  
37  
38  
39  
40  
41  
42  
43  
44  
45  
46  
47  
48  
49  
50  
51  
52  
53  
54  
55  
56  
57  
58  
59  
60  
61  
62  
63  
64  
65

698 Zhou, T., Nijssen, B., Gao, H., & Lettenmaier, D. P. (2016). The Contribution of Reservoirs to  
699 Global Land Surface Water Storage Variations. *Journal of Hydrometeorology*, 17(1), 309–  
700 325. <https://doi.org/10.1175/JHM-D-15-0002.1>

701  
702

## 7. Appendix

### 7.1. River-regulation algorithm ResORR tested in a theoretical two-reservoir system using synthetic data

A theoretical two inter-connected linear reservoir system with artificially generated headwater flow inputs was used to test the theoretical robustness of the mass conserving and numerical stability of the ResORR algorithm. This classic problem (Figure 8) also helped visualize the outputs of ResORR algorithm and verify if mass balance is maintained.

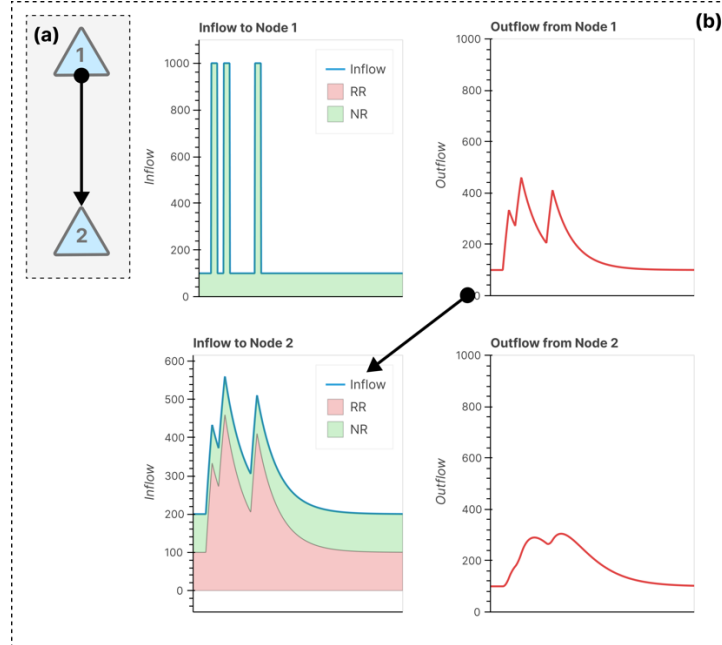


Figure 8: (a) Schematic showing the two-reservoir system setup. The black arrow denotes the direction of flow of water. (b) Hydrographs showing inflow and outflow from nodes 1 and 2. In this case, three input pulses of  $1000 \text{ L}^3/\text{T}$  units were fed into node 1, and its outflow was treated as the inflow to the downstream node 2. The inflow and outflow at node 2 represent the ‘theoretical’ answer for the ResORR algorithm to be theoretically valid.

A system of two interconnected linear reservoirs were set up, like the schematic shown in Figure 8. To understand how the outflow from an upstream reservoir would affect the inflow to the downstream reservoir, we first generated a synthetic headwater inflow hydrograph for reservoir 1 and then applied ResORR to predict the regulated inflow to the downstream reservoir at node 2. Both the reservoirs were provided with a constant water influx of  $100 \text{ L}^3/\text{T}$  units in the form of natural runoff, NR. Additionally, the upstream reservoir, at node 1, was provided with three pulses of high inflow volumes of  $1000 \text{ L}^3/\text{T}$  units. The reservoirs were treated as linear reservoirs, where the outflow from a reservoir at any given time as a linear function of the instantaneous storage, and can be defined as follows –

$$O = K \times S$$

Where,  $K [T^{-1}]$  is the reaction factor, which determines how quickly the reservoir drains ( $K = 0.01$  in this experiment). The outflow from the upstream reservoir at node 1 was then treated as the regulated runoff, RR for the downstream reservoir, node 2. Using the inflows and outflows

obtained at both the reservoirs, the storage change was obtained using (5). The theoretical natural runoff, TNR, was also obtained using (3). The ResORR was then run using this simulated storage change and TNR information as inputs, to model the inflow at both the reservoirs. The modeled inflow of ResORR was then compared with the synthetically generated inflow at the downstream node 2, with a perfect match between them. The closure of water balance was also tested by comparing the total inflow volumes in the modeled and synthetic inflow.

## 7.2. Performance metrics used for assessing ResORR

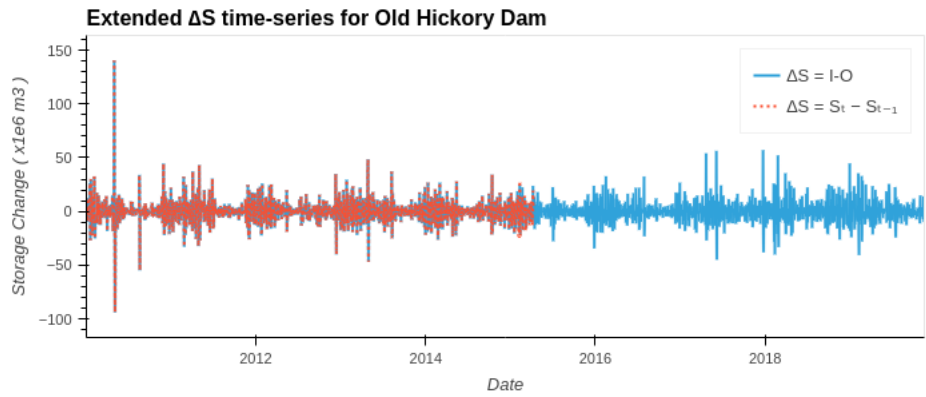
The following five commonly used performance metrics were used in this study to quantify the skill of the river regulation model -

Metric	Equation	Description
Nash-Sutcliffe Efficiency (NSE) (Nash & Sutcliffe, 1970)	$1 - \frac{\sum_{t=1}^T (Q_O^t - Q_M^t)^2}{\sum_{t=1}^T (Q_O^t - \overline{Q_O})^2}$ <p>Where, <math>Q_O^t</math> and <math>Q_M^t</math> are observed and modeled streamflow respectively. <math>\overline{Q_O}</math> is the mean observed streamflow.</p>	The NSE can vary between $-\infty$ and 1. A value of 1 indicates a perfect match between observed and modeled values. A value of 0 indicates that the model predictions are as performant as using the mean of the observed values as a predictor. Higher values are better.
Kling-Gupta Efficiency (KGE) (Gupta et al., 2009)	$1 - \sqrt{(r - 1)^2 + (\alpha - 1)^2 + (\beta - 1)^2}$ <p>Where, <math>r</math> is the linear correlation between modeled and observed values, <math>\alpha = \left(\frac{\sigma_M}{\sigma_O} - 1\right)^2</math>, <math>\sigma_M</math> and <math>\sigma_O</math> are the standard deviations of the modeled and observed values, <math>\beta = \left(\frac{\mu_M}{\mu_O} - 1\right)^2</math>, <math>\mu_M</math> and <math>\mu_O</math> are mean modeled and observed values.</p>	The KGE varies between $-\infty$ and 1. A value of -0.41 indicates model performance equal to using the mean of the observed values as a predictor (Knoben et al., 2019). Higher values are better.
Pearson's R	$\frac{cov(Q_O, Q_M)}{\sigma_O \sigma_M}$ <p>Where, <math>cov(Q_O, Q_M)</math> is the covariance of the observed and modeled values. <math>\sigma_M</math> and <math>\sigma_O</math> are the standard deviations of the modeled and observed values</p>	The Pearson's R can vary from -1 to 1, where 1 indicates a perfect positive linear correlation. A value of 0 indicates no correlation.
Normalized Root-Mean Squared Error (NRMSE)	$\frac{\sqrt{\frac{\sum_{i=1}^N (Q_O - Q_M)^2}{N}}}{\max(Q_O) - \min(Q_O)}$ <p>Where, <math>\max(Q_O)</math> and <math>\min(Q_O)</math> are the maximum and minimum observed streamflow values.</p>	The NRMSE represents the standard deviation of the residuals as a fraction of the range of the observed values. Lower values are better.

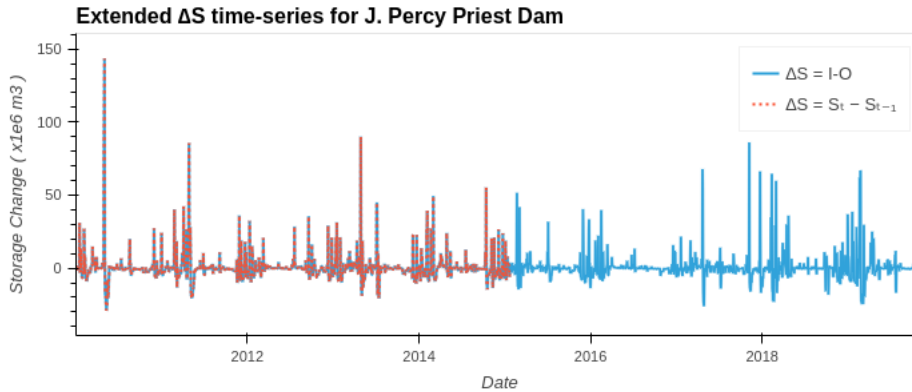
<p>Normalized Mean Absolute Error (NMAE)</p>	$\frac{\sum_{i=1}^N  Q_M - Q_O }{\max(Q_O) - \min(Q_O)}$ <p>Where, <math>N</math> is the number of observations, <math> Q_M - Q_O </math> is the absolute difference of modeled and observed values</p>	<p>The NMAE represents the average absolute difference between observed and modeled values as a fraction of the range of observed values. Lower values are better.</p>
--	---	--

738 **7.3. Handling missing In-situ storage data**

739 Two dams in the basin, Old Hickory and Laurel, had missing in-situ storage data after April  
 740 2015, due to which storage change could not be calculated using observed (in-situ) storage. This  
 741 missing data was filled by assuming water mass-balance owing to inflow and outflow from the  
 742 reservoirs,  $\Delta S = I - O$ .



743



744

745